Journal of Hazardous Materials 194 (2011) 15–23

Contents lists available at ScienceDirect

Journal of Hazardous Materials

journal homepage: www.elsevier.com/locate/jhazmat

Chromate reduction in Fe(II)-containing soil affected by hyperalkaline leachate from chromite ore processing residue

Robert A. Whittleston[a], Douglas I. Stewart[b,*], Robert J.G. Mortimer[a], Zana C. Tilt[a], Andrew P. Brown[c], Kalotina Geraki[d], Ian T. Burke[a,*]

[a] School of Earth and Environment, University of Leeds, Leeds LS2 9JT, UK
[b] School of Civil Engineering, University of Leeds, Leeds LS2 9JT, UK
[c] School of Process, Environmental and Materials Engineering, University of Leeds, Leeds LS2 9JT, UK
[d] Diamond Light Source, Harwell Science and Innovation Campus, Didcot, Oxfordshire OX11 0DE, UK

ARTICLE INFO

Article history:
Received 17 March 2011
Received in revised form 14 June 2011
Accepted 18 July 2011
Available online 5 August 2011

Keywords:
Chromium
COPR
Natural attenuation
Cr-speciation
Cr(VI) contaminated soils and groundwater

ABSTRACT

Highly alkaline (pH 12.2) chromate contaminated leachate (990 μmol L^{-1}) has been entering soils below a chromite ore processing residue disposal (COPR) site for over 100 years. The soil immediately beneath the waste has a pH of 11 → 12.5, contains 0.3 → 0.5% (w/w) chromium, and 45 → 75% of the microbially available iron is Fe(II). Despite elevated pH, a viable microbial consortium of *Firmicutes* dominated iron reducers was isolated from this COPR affected soil. Soil pH and Cr concentration decrease with distance from the waste. XAS analysis of soil samples indicated that Cr is present as a mixed Cr(III)–Fe(III) oxyhydroxide phase, suggesting that the elevated soil Cr content is due to reductive precipitation of Cr(VI) by Fe(II). Microcosm results demonstrate the capacity of COPR affected soil to abiotically remove all Cr(VI) from the leachate within 40 days. In air oxidation experiments less than 2% of the total Cr in the soil was remobilised despite significant Fe(II) oxidation. XAS analysis after air oxidation showed no change in Cr-speciation, indicating the Cr(III)-containing phase is a stable long term host for Cr. This work suggests that reductive precipitation of Cr(VI) is an effective method of contaminant immobilisation in soils where microbially produced Fe(II) is present.

© 2011 Elsevier B.V. All rights reserved.

1. Introduction

Chromium is a widely used industrial metal extracted commercially from the mineral chromite. Chromite ore is processed by roasting with an alkali-carbonate at 1150 °C to oxidise insoluble Cr(III) to soluble Cr(VI) which is extracted with water upon cooling. Traditionally, limestone was added to the reaction to improve air penetration, and this "high-lime" process was the primary commercial method of chromium production up to the 1960s [1]. Although now superseded by lime-free processes, high-lime Cr extraction recently accounted for 40% of Cr production worldwide [1]. The process is inefficient, and is responsible for producing large quantities of waste (600,000 t yr^{-1} in 2001 [1]) known as chromite ore processing residue (COPR). COPR from the high-lime process is highly alkaline and typically contains 2–7% total chromium by weight [2–4], and although much is unreacted insoluble chromite ore (i.e. Cr(III)), up to 30% can be in the oxidised Cr(VI) form [4]. Water in contact with COPR has a pH of 11 → 12, and can contain up to 1.6 mmol L^{-1} Cr(VI) as the highly mobile and toxic anion chromate [4].

Poorly controlled landfilling of COPR is a global problem [1,3], and locally such sites can be major sources of pollution. Remediation of COPR legacy sites is challenging because they are often in urban areas and date from times when COPR disposal was poorly managed [5]. Traditional "dig and dump" remediation strategies are costly due to the large volumes involved, and inadvisable due to the risk of forming carcinogenic Cr(VI) bearing dusts [6,7]. In contrast to the harmful properties of Cr(VI), the reduced Cr(III) form is an essential trace nutrient in plants and animals [8,9], readily sorbs to soil minerals, and (co)-precipitates as insoluble Cr(III) hydroxides in neutral and alkaline environments [9,10].

In natural environments a number of chemical species are known to reduce Cr(VI), including Fe(II), organic matter and sulphide [11]. In anaerobic soils Fe(II) is probably the most important, as iron is abundant and microbial reduction of Fe(III) occurs as anoxia develops [12–15]. Cr(VI) is readily reduced by oxidation of Fe(II) [9], and as Cr(III) can substitute for Fe(III), the resulting Cr(III) is likely to be incorporated into iron(III) oxyhydroxides [16]. However, such metastable iron oxyhydroxides can exhibit high bioavailability [17] and thus Fe(II)/Fe(III) cycling may continue in environments where microbial iron reduction can occur. Iron

* Corresponding authors.
E-mail addresses: d.i.stewart@leeds.ac.uk (D.I. Stewart), i.burke@see.leeds.ac.uk (I.T. Burke).

0304-3894/$ – see front matter © 2011 Elsevier B.V. All rights reserved.
doi:10.1016/j.jhazmat.2011.07.067

cycling is likely to be important at COPR sites as a broad range of microbes have adapted to allow them to respire and grow in high pH and metal contaminated environments [15,18–20].

This paper describes a site in the North of England where COPR has been deposited next to a canal on the side of a valley and close to a river in the bottom [21]. It is of environmental concern because water emerging from the waste pile, which enters both the groundwater and surface water systems, has an elevated Cr(VI) concentration [21]. Previous investigations have found that the anoxic soils beneath the waste have accumulated Cr [21,22]. These studies suggest that microbially mediated reduction of COPR derived chromate is naturally attenuating contaminant transport. Here we use a combination of field investigation, microcosm experiments, microbial community analysis and X-ray absorption spectroscopy to investigate the controls on geochemical transformation of Cr(VI) in COPR contaminated water as it enters underlying anoxic soil horizons.

2. Materials and methods

2.1. Field sampling and sample handling

A 19th century COPR tip is located in the North of England. It is in a glacial valley, through undifferentiated siltstone and mudstone, in-filled with alluvial deposits (Fig. 1a; see also [21,22]). A thin layer of topsoil covers much of the tip, however to date no chemical remediation strategy has been employed at the site. Soil samples were collected in March 2009 from six boreholes in a line away from the tip using a hand auger and 1 m core sampler (Fig. 1b and c). Water was taken from a standpipe in BH5 screened into the COPR using a PVC bailer (BH5 dates from a 2002 commercial site investigation, Fig. 1b). Samples were stored at 4 °C in the dark in sealed polythene containers (XAS samples were stored at −80 °C in glass vials). Sealed containers with samples for microbial community analysis were stored anaerobically using Anaerogen™ sachets.

2.2. Sample characterisation

Soil samples were characterised using X-ray powder diffraction (XRD), X-ray fluorescence (XRF), total organic carbon analysis, pH analysis, deionised water (DIW) soluble Cr(VI) content, scanning electron microscopy (SEM) and scanning transmission electron microscopy (STEM) using standard protocols [23–25] (see Supporting Information). Water chemistry was determined using the standard methods below.

2.3. Reduction microcosm experiments

Triplicate microcosms were prepared using 10 g of homogenised soil from sample B2-310 and 100 ml of COPR leachate in 120 ml glass serum bottles [22]. After sealing, the headspace was purged with nitrogen. A sterilised control was prepared by autoclaving soil with a nitrogen purged headspace (120 °C, 20 min) and filter sterilised COPR leachate added upon cooling. Bottles (incubated in the dark at 21 °C) were periodically sampled aseptically for geochemical analysis. During sampling microcosms were shaken and 3 ml soil slurry extracted. Samples were centrifuged (3 min, 16,000 × *g*) and the water analysed for, pH, Eh and Cr(VI), and soil for acid extractable Fe(II).

2.4. Geochemical methods

Eh and pH were measured using an Orion meter (pH calibrated at 7 and 10). UV/VIS spectroscopy methods based on reactions with diphenycarbazide and ferrozine were used to determine aqueous Cr(VI) and Fe concentrations using a Cecil CE3021 UV/VIS Spectrophotometer [26,27], with standard calibrations performed regularly. As a proxy for microbial available Fe [28,29], the percentage Fe(II) in the soil was determined after extraction by 0.5 N HCl and reaction with ferrozine [30].

2.5. Oxidation experiments

DIW equilibrated with atmospheric O_2 and CO_2 was used as a proxy for rain water in leaching tests that evaluated the potential for Cr remobilisation. 500 ml conical flasks containing 10 g B2-310 soil and 100 ml DIW were left open to the atmosphere using a foam bung, placed on an orbital shaker (150 rpm), and incubated in the dark at 21 °C. Duplicate experiments were sampled periodically over 60 days. At each sample point, 1.5 ml soil slurry was extracted using a sterile syringe, and centrifuged (3 min 16,000 × *g*). The supernatant was then analysed for pH, Eh aqueous Cr(VI) concentration, and the soil pellet analysed for Fe(II) in solids, as described above.

2.6. X-ray absorption spectroscopy (XAS)

XANES and EXAFS spectra were collected on station I18 at Diamond Light Source, UK, from seven soil samples from below the local water table and the B2-310 oxidation sample. Spectra were compared to standard laboratory chemicals, natural chromite ore, and amorphous Cr-hydroxide (precipitated by dropwise neutralisation of $CrCl_3$ solution using NaOH [31]). XANES and EXAFS spectra were summed and normalised using Athena v0.8.056. Background subtracted EXAFS spectra were prepared for selected B2 and B3 samples using PySpline v1.1, and were modelled using DLexcurv v1.0 with improvement in *R* value used to measure fit (see S.I. for details).

2.7. Culturing of iron reducers

An alkaline (pH 9.2) growth media was used to culture a consortium of Fe(II)-reducing anaerobes. Fe(III) citrate and yeast extract were used as sole electron acceptors and donors (see S.I. for details.). 5 mL of B2-310 soil in sterile growth media (20 g L^{-1}) was sealed into 10 mL glass serum bottles with nitrogen headspace. The resulting culture was progressed repeatedly to obtain a viable consortium. Precipitate colour change from orange to black indicating Fe(II) production was confirmed using the method described above.

2.8. Microbial community analysis

Microbial DNA was extracted from B2-310 and the Fe(III)-reducing culture. A 16S rRNA gene fragment (∼500 bp) was amplified from each sample by polymerase chain reaction (PCR) using broad specificity primers. The PCR product was ligated into a standard cloning vector, and transformed into *E. coli* competent cells to isolate plasmids containing the insert, which were sent for sequencing (see S.I. for details). The quality of each gene sequence was evaluated, and non-chimeric sequences were classified using the Ribosomal Database Project (RDP) naïve Bayesian Classifier [32] in August 2010 (GenBank accession numbers FR695903–FR695964, and FR820910–FR820956).

3. Results

3.1. Ground investigation

Borehole B1 (Fig. 1b) penetrated a topsoil layer and encountered COPR waste at 55 cm but did not enter the underlying soil. B2 penetrated a thicker topsoil layer before entering COPR waste at

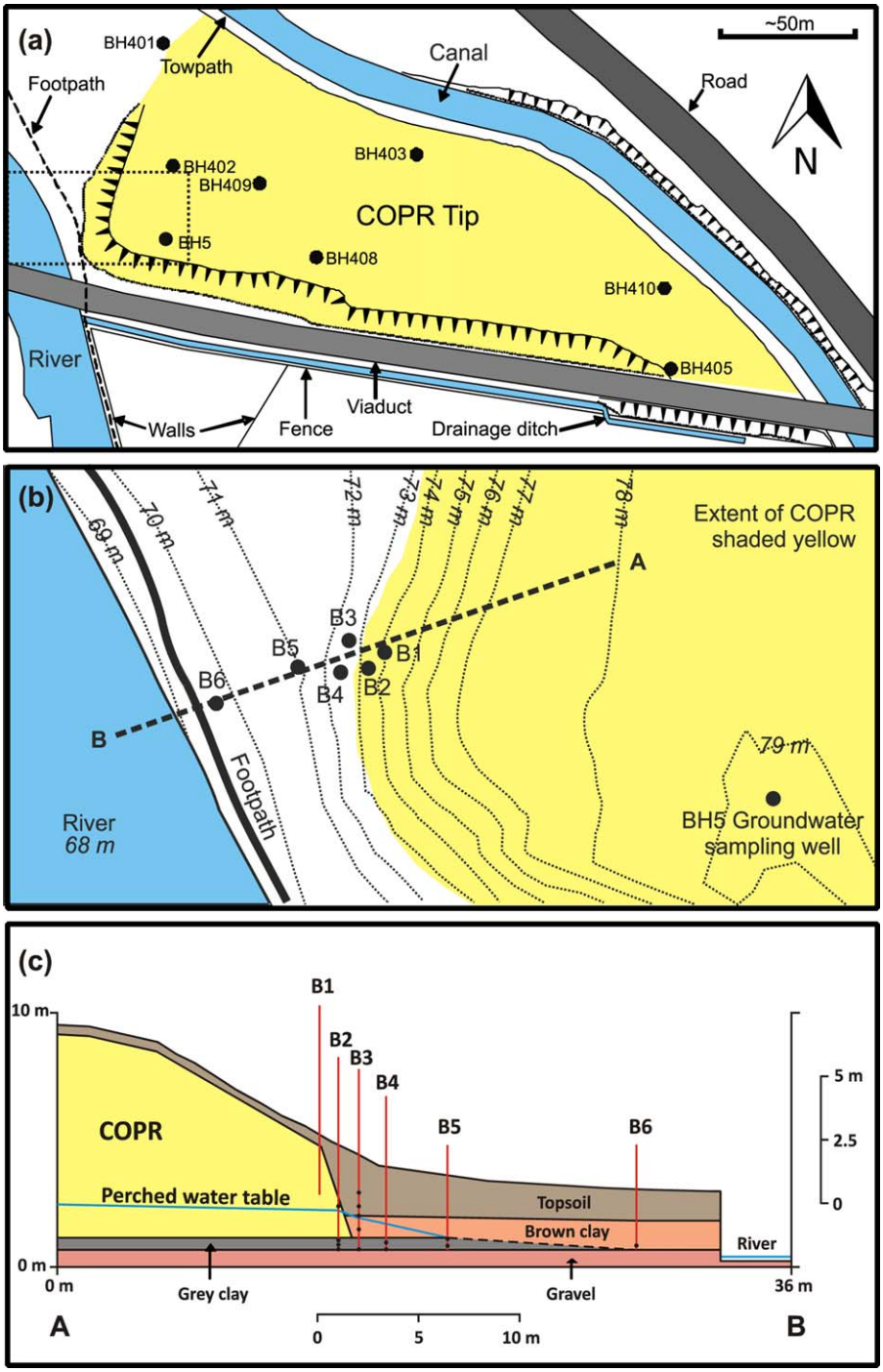

Fig. 1. (a) Sketch map of the site indicating the study area and the borehole locations from commercial site investigations undertaken in 2002 and 2007, (b) the study area on south western edge of the waste showing the new borehole locations, and (c) conceptual ground model along line of pseudo-section.

190 cm, grey sandy clay at 310 cm, and terminated in a gravel layer at 365 cm. Subsequent boreholes B3 → B6 (in order of distance from the waste edge), did not go through the COPR waste, but revealed a sequence of topsoil over brown sandy clay, then grey sandy clay, and terminated in the gravel layer. The pH of water in the COPR (BH5) was 12.2 and the Cr(VI) concentration was 990 μmol L^{-1} (51.5 mg l^{-1} as CrO_4^{2-}).

3.2. Sample characterisation

The properties of COPR and soil samples are shown in Table 1, and full XRF analysis is presented in Table S1 (Supporting Information). The COPR sample (B2 190–210) contained 1.27% (w/w) chromium, and 119.1 mg kg^{-1} of Cr(VI) was leachable with DIW (see Stewart et al. [21] for full characterisation COPR leachate). The soil samples from closest to the COPR contained between 0.3 and 0.5% (w/w) chromium (samples B2-310 and B2 320–340 from the grey clay immediately beneath the COPR, and B3 150–200 and B3 200–240 from the topsoil immediately next to the COPR). Backscatter SEM images of grey clay sample (B2-310) show it to consist of a largely fine grained matrix, interspaced with angular quartz grains (S.I., Fig. S1). The mean Cr-concentration within fine matrix determined by SEM microprobe was 0.46 ± 0.29% (w/w), consistent with the bulk XRF analysis (0.34%, w/w) for this sample. The amount of

Table 1
Soil composition.

Borehole	Depth (cm)	Soil type	Total Cr (mg kg^{-1})	Leachable Cr(VI) (mg kg^{-1})	pH	% Acid extractable iron as Fe(II)	Major minerals present	Water strike	TOC (%)
B2	190–210	COPR waste	12,716	119.10	12.51	–	Portlandite	No	0.26
	310	Grey clay	3436	6.65	12.16	53	Quartz, Kaolinite, Albite	Yes	0.96
	320–340	Grey grey	3946	4.54	12.51	45	Quartz, Kaolinite	Yes	0.96
	365	Grey clay	846	5.80	11.2	75	Quartz, Kaolinite, Illite	Yes	0.50
B3	150–200	Topsoil	4890	8.76	4.31	4	–	No	13.38
	200–240	Topsoil	4321	1.45	7.03	5	–	No	14.47
	240–250	Brown clay	1431	0.89	7.96	5	Quartz, Kaolinite, Illite	Yes	1.86
	280–335	Brown clay	1511	0.46	7.76	37	Quartz, Kaolinite	Yes	0.54
	360–365	Grey clay	1379	0.46	7.83	31	–	Yes	0.23
B4	240–270	Grey clay	336	0.60	6.58	68	Quartz, Kaolinite	Yes	1.16
	270–280	Grey clay	847	0.60	6.59	92	–	Yes	0.25
B5	190–200	Brown clay	1599	0.74	7.2	60	–	No	0.23
	220–230	Grey clay	1278	0.89	6.62	89	–	No	0.36
B6	220	Brown clay	162	1.59	5.64	N.d.	Quartz, Kaolinite	No	0.14

–, Not determined; N.d., Not detected.

chromium in the soil samples shows a rough trend of decreasing with depth in B2 and B3, and of decreasing with horizontal distance from the waste pile (B3 > B4 > B6). These trends are reflected in pH, with the samples closest to the COPR having the highest values, which were above pH 12 immediately below the waste in B2. The percentages of iron extracted by 0.5 N HCl present as Fe(II) in B2 soils from immediately below the waste were 45 → 75%, and values were similar throughout the grey clay layer. In the overlying brown clay and topsoil layers percentages of iron extracted by 0.5 N HCl present as Fe(II) were more variable but generally increased with depth. This suggests that Fe(III) reducing conditions develop rapidly under saturated conditions.

XANES spectra from a selection of grey and brown clay samples taken from boreholes with increasing distance from the COPR all lacked the characteristic pre-edge feature associated with Cr(VI) at 5994 eV [33] (Fig. 2). All XANES spectra indicate that Cr is present predominately in the reduced Cr(III) form although minor amounts of Cr(VI) (up to 3–5% of the total Cr depending on sample concentration) may not be detected in XANES spectra [34]. The amount of DIW leachable Cr(VI) in the soil samples (Table 1) falls below this detection limit, thus XANES and DIW leaching tests bracket the amount of Cr(VI) within these soils at approximately 0.5–3% of the total Cr. Due to the suspected presence of freshly precipitated Cr(III) hydroxides in these soils, estimates of Cr(VI) content from alkaline extractions were excluded as significant method induced oxidation of Cr(III) was observed in these samples [25]. Although XANES spectra from many Cr(III) compounds are superficially similar, the chromite ore spectrum has a distinct shoulder at approximately 6003 eV which is absent in the less crystalline Cr(III) hydroxide spectrum. The spectra from the soil samples do not have this shoulder.

EXAFS spectra from selected samples were fitted with a shell of 6 oxygen atoms at 1.97 → 1.99 Å and refined to minimise *R*. The spectral features beyond 2 Å were fitted with a further 3 shells of Fe(Cr) backscatters at 3.06 → 3.07 Å, 3.30 → 3.34 Å and 3.93 → 4.02 Å, and further refined (Table 2, n.b. Fe and Cr backscatters are indistinguishable in EXAFS modelling [35]). EXAFS and Fourier transformed EXAFS spectra are shown in Fig. 3.

To further investigate the co-localisation of Cr at the nanoscale, STEM analysis was carried out on sample B2-310. Dark field STEM imaging identified fine-grained aggregates amongst coarser grained material (Fig. 4). EDX point analysis shows Cr and Fe co-localisation in the fine-grained region (Fig. 4A, point 1; EDX spectrum 1 in S.I. Fig. S2). Bright field TEM imaging (Fig. 4B) con-

Table 2
EXAFS model fitting parameters where *n* is the occupancy (±25%), *r* is the interatomic distance (±0.02 Å for the first shell, ±0.05 Å for outer shells), $2\sigma^2$ is the Debye–Waller factor (±25%), and *R* is the least squares residual.

Sample	Shell	*n*	*R* (Å)	$2\sigma^2$ (Å^2)	*R*	% gain
B2 310–320	O	6	1.99	0.011	49.2	
	Fe(Cr)	2.9	3.06	0.013		
	Fe(Cr)	3.3	3.34	0.010		
	Fe(Cr)	3.3	3.99	0.014	30.1	38.7
B2 320–340	O	6	1.98	0.011	42.9	
	Fe(Cr)	3.1	3.07	0.017		
	Fe(Cr)	3.1	3.33	0.020		
	Fe(Cr)	3.1	3.97	0.022	28.1	34.5
B2 310 oxidised	O	6	1.98	0.010	42.9	
	Fe(Cr)	3.1	3.06	0.014		
	Fe(Cr)	3	3.33	0.020		
	Fe(Cr)	3.4	3.99	0.022	28.2	34.2
B3 200–240	O	6	1.97	0.010	43.3	
	Fe(Cr)	3	3.07	0.018		
	Fe(Cr)	2.9	3.32	0.012		
	Fe(Cr)	3.1	3.93	0.016	30.4	29.9
B3 240–250	O	6	1.99	0.010	40.9	
	Fe(Cr)	3	3.07	0.011		
	Fe(Cr)	3	3.30	0.011		
	Fe(Cr)	3	4.02	0.026	30.6	25.1

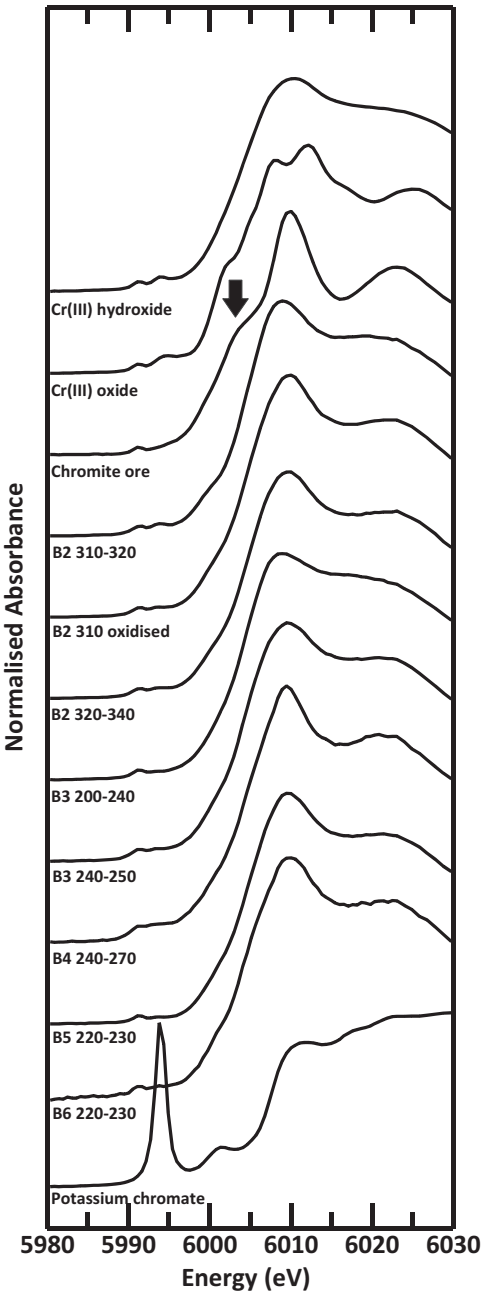

Fig. 2. Normalised chromium K-edge XANES spectra collected from soil samples and synthetic standards. Arrow indicates a distinctive curve inflection present at 6003 eV in the chromite ore spectra.

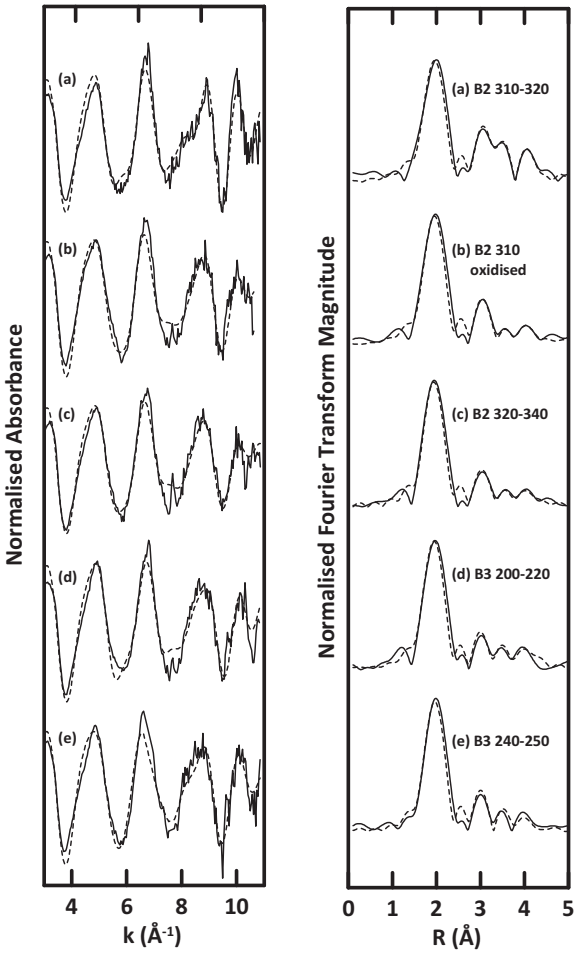

Fig. 3. Chromium K-edge EXAFS spectra collected from selected soil samples (left) and corresponding Fourier transformations (right). Dashed lines represent model fits produced in DLexcurv v1.0 using the parameters listed in Table 2.

firms that the Fe and Cr containing material consists of 5–10 nm sized particles. STEM-EDX elemental mapping of this area (Fig. 4) shows Cr (Kα X-rays) localised with Fe in the fine grained region, Al and Si are localised in the surrounding larger particles. EDX point analysis of a crystalline Fe-rich particle (Fig. 4A, point 2; EDX spectrum 2, Fig. S2) and a Si and Al rich particle (Fig. 4A, point 3; EDX spectrum 3, Fig. S2) confirmed the lack of Cr in these regions.

3.3. Reduction microcosm experiments

The microcosm experiments investigated the interaction of COPR leachate with Fe(II)-containing grey clay from below the waste pile (sample B2-310). The initial pH value of microcosms was 12.2, while the corresponding sterile control had an initial pH value of 12. The pH in all microcosms decreased over about 20 days before levelling off at 11.7 (Fig. 5). At the first sample point (~1 h) the aqueous Cr(VI) concentration had dropped from the leachate value of 990 to $788 \pm 14\ \mu mol\ L^{-1}$, and Cr(VI) was subsequently removed from solution over the first 30 days in all microcosm bottles. The concentration of Cr(VI) in the corresponding sterile control was $822\ \mu mol\ L^{-1}$ at 1 h and Cr(VI) was also completely removed from solution by 14 days. At the first sample point 36% of the 0.5 N HCl extractable iron in the microcosms was present as Fe(II), and by day 4 this had dropped to 30% at the same time as most of the Cr(VI) was removed ($788 \rightarrow 257\ \mu mol\ L^{-1}$). Percentage 0.5 N HCl extractable Fe as Fe(II) then remains within error of the 4 day value. The percentage of the 0.5 N HCl extractable iron in the sterile control as Fe(II) was 45% with no significant change during the experiments. Eh values at the first sampling point were -77 ± 10 and -65 mV for the active microcosms and sterile control, respectively, and decreased very slowly to -135 ± 40 and -185 mV at 83 days. Aqueous Fe remained at between 2 and 10 $\mu mol\ L^{-1}$ in all microcosms throughout the duration of the incubations.

3.4. Microbial community analysis

The 62 16s rRNA gene sequences obtained from B2-310 soil were assigned to 9 different bacterial phyla (confidence threshold >98%) with approximately 10% left unassigned. Three phyla were dominant, with 52%, 19%, and 16% of sequences assigned to *Proteobacteria*, *Firmicutes* and *Bacteriodetes*, respectively (S.I.,

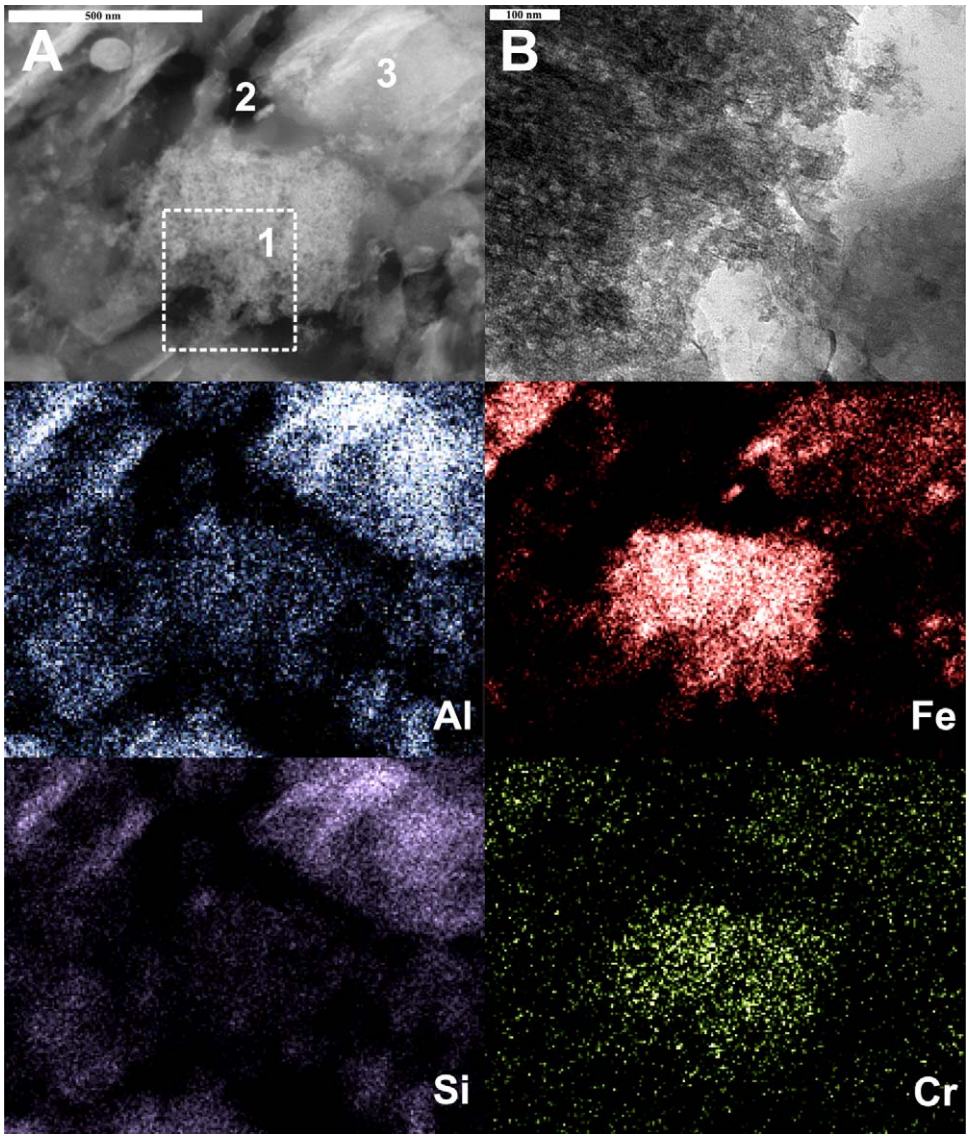

Fig. 4. TEM images and corresponding STEM-EDX elemental maps of B2-310 soil. (A) Darkfield TEM image with locations of point EDX measurements, marked 1–3 (scale bar 500 nm); (B) Higher magnification bright field TEM image of fine-grained area highlighted in (A), rotated 90° (scale bar 100 nm). STEM-EDX maps of elemental distribution of aluminium ($K\alpha$ X-ray energy), iron ($K\alpha$), silicon ($K\alpha$) and chromium ($K\alpha$).

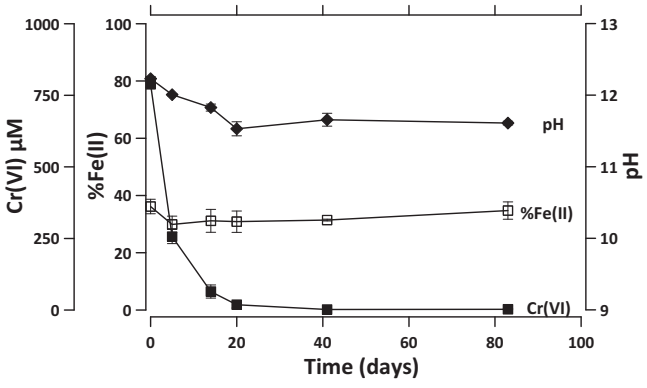

Fig. 5. Microcosm experiments; (■) aqueous Cr(VI); (♦) pH; (□) % of 0.5 N HCl extractable Fe as Fe(II) in soils. Error bars are one standard deviation from the mean of triplicate experiments. Sterile data not shown.

Table S2). When this soil was incubated in an alkaline Fe-reducing media a microbial consortium was cultured that survived repeated progressions. The 16s rRNA gene sequences recovered from this consortium were dominated by the phylum *Firmicutes* (91% of the 47 sequences), with just 2% assigned to *Proteobacteria* and 7% left unassigned (S.I., Table S3). Of the *Firmicutes* sequences in this consortium, all were found to be members of the *Clostridiales* order with representatives identified to genus level that were also found in the original soil sample, such as *Anaerobranca* and *Tissierella.*

3.5. Oxidation experiments

An aqueous suspension of soil sample B2-310 was oxidised for 60 days with deionised water in equilibrium with atmospheric O_2. After 14 days of oxidation 1.5% of the total Cr within the soil was remobilised as Cr(VI) and no further remobilisation occurred for the remainder of the 60 days experiment (Fig. 6). The % of 0.5 N HCl extractable iron that was Fe(II) decreased, the Eh increased from -37 ± 15 mV to $+202 \pm 33$ mV, and aqueous Fe decreased from 31 ± 23 µmol L^{-1} to 11 ± 2 µmol L^{-1} over the course of the

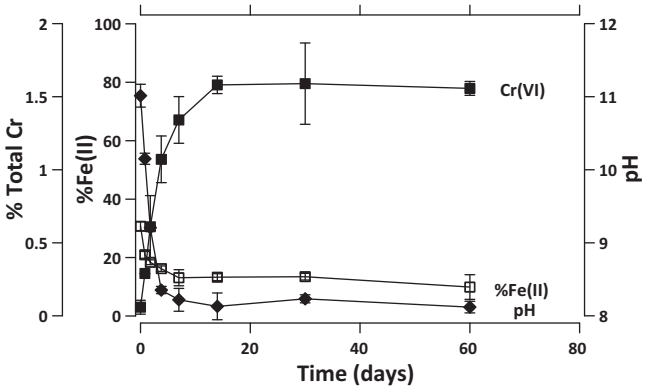

Fig. 6. Air oxidation experiments; remobilisation of Cr(VI) to solution as a percentage of total Cr (■); pH (♦); % of 0.5 N HCl extractable iron as Fe(II) (□). Error bars are the range of the duplicate experiments.

experiment. The pH dropped rapidly from an initial value of 11 to just above 8 after 4 days, and then remained steady about this value.

4. Discussion

4.1. Ground model

Data from the six boreholes advanced during this project were used to further develop the existing ground model for the site (Fig. 1c). They confirm COPR waste has been placed directly over the alluvial soils and then covered with topsoil. The relationship between the brown clay and the COPR indicates that it is made ground that was placed after COPR tipping. The grey clay, which was absent in B6 closest to the river, is thought to have been the surface layer prior to COPR tipping. The gravel layer is part of the alluvial deposits that underlie the entire site. Data from a confidential commercial site investigation conducted in 2007 (locations shown in Fig. 1a) support the proposed ground model, and reveal that the alluvial deposits are ~8 m thick. A hydrogeology study in April 2009 [36] revealed that there is a perched water table in the waste just over 2 m above the underlying water table in the alluvial deposits, and that the underlying flow in the alluvial deposits is roughly south-westerly from the valley side towards the river. Together, the local lithology, the perched water table and the direction of underlying flow indicated that water flow from the COPR tip is initially downward and then towards the river roughly along the pseudo-section in Fig. 1b.

4.2. Distribution and speciation of Cr in soils

The general trend in the borehole data (Table 1) is that the Cr concentration in the soil decreases with distance from the waste. The variation in the Cr content of samples from B4 and B5 is counter to the general trend, but this may be attributed to non-uniform flow of contaminated water as it migrates away from the tip. Furthermore, B4 and B5 are slightly offset laterally in opposite directions from the line of the pseudo section (Fig. 1b), and thus may have received slightly different influent water. The trend can be explained either by transport of waste particles into the soil or by interaction with a plume of Cr(VI) containing leachate. Cr(III) in COPR is found predominately in unreacted chromite ore particles [4,21,37]. However, XANES analysis suggest that Cr is present in the soil predominately as a poorly crystalline Cr(III) phase (Fig. 2). EXAFS spectra from samples close to the waste also lack the spectral features characteristic of chromite samples (there are no sub peaks at $K = 5.1$ and 8 $Å^{-1}$, Supporting Information, Fig. S3) and the coordination environment is inconsistent with chromite Cr–Fe bond distances [38–40] (Supporting Information, Table S4).

The Cr(III) coordination environment in all samples with EXAFS analysis was fitted with 6 oxygen atoms at 1.97 → 1.99 Å, indicating octahedral Cr–O coordination. Further shells of Fe(Cr) atoms at distances of 3.06 → 3.07 and 3.30 → 3.34 Å from the central Cr atom are characteristic of the edge and double corner octahedral sharing geometries present in Cr(III) substituted iron oxy-hydroxides [17,35,41,42]. The presence of an additional shell of backscatters at 3.93 → 4.02 Å could indicate that single corner sharing geometries are present in surface precipitation of γ-CrOOH on hydrous ferric oxides [41]. γ-CrOOH also has a Cr–Cr edge sharing bond distance of 3.06 Å [41]. Therefore the Cr(III) coordination resolved by EXAFS analysis of soil samples can be best described as that of a poorly ordered Cr–Fe–OOH precipitate containing both incorporated and surface precipitated Cr(III). This interpretation is supported by the STEM analysis of B2-310 soil (Fig. 4), which found that Cr was associated with 5–10 nm sized Fe-rich particles. Identification of this mixed Cr(III)–Fe(III) oxy-hydroxide phase indicates that chromium in soils receiving water from the COPR waste is not the result of transport of chromite particles from the waste, and therefore, is most likely the result of *in situ* reduction of Cr(VI) from the contaminated groundwater by reaction with Fe(II).

4.3. Reduction of Cr(VI) in microcosms

The microcosm experiments show that soil from B2-310 is capable of removing Cr(VI) from the COPR leachate. Cr(VI) reduction was observed in both sterile and non sterile microcosms indicating that the reaction was abiotic (Fig. 5). At pH values greater than 6 the most likely abiotic removal mechanism is reduction to Cr(III) by soil associated Fe(II) followed by precipitation [11]. The percentage of Fe(II) in the 0.5 N HCl extractions reduced slightly during the incubation which is compatible with Fe(II) being consumed by reaction with the Cr(VI), although the overall change is within the measurement error. This minor reduction in Fe(II) during Cr(VI) removal is consistent with the calculated Fe(II): Cr(VI) ratio of 20–30:1 present in these experiments.

4.4. Capacity for Fe(III)-reduction in alkaline soils

Bioreduction of Fe(III) oxides is commonplace in water saturated soils containing organic matter. The elevated pH and Cr(VI) conditions existing at this site provide additional challenges to microbial respiration. Despite this, a relatively diverse microbial community was characterised from soil B2 310. Many of the sequences in this community are best database matches to bacteria isolated from studies of high pH tufa and soda lake environments [43,44], as well as unidentified sequences from other COPR affected environments [5,21].

The isolation of a community of microorganisms capable of Fe(III) reduction from B2-310 soil clearly shows that this soil contains indigenous microorganisms capable of iron reduction. Around 40% of the 0.5 N HCl extractable Fe present in B2-310 soil is Fe(II), despite the constant exposure to a Cr(VI) flux for over 100 years, which indicates that there must be a mechanism for replenishing Fe(II) within this soil. Taken together, these facts strongly suggest microbial iron reduction is responsible for the Fe(II) present in the soil and, by implication, is indirectly responsible for the reductive precipitation of Cr(VI). The relative dominance of the *Firmicutes* sequences in the consortium extracted by growth in alkaline Fe(III)-citrate media (S.I., Table S3), when compared to the population from the original soil, suggests that members of this phylum are responsible for the Fe(III) reducing capacity. The indigenous population of B2-310 soil did not induce Fe(II) accumulation in soil microcosms at pH 12 where soil organic matter was available as an electron donor

(~1% TOC, Table 1), indicating that the microbial mechanism for producing the Fe(II) at high pH is either slow or was not reproduced successfully in these homogenised systems.

4.5. Soil oxidation experiments

During oxidation of B2-310 soil only a small amount of Cr(VI) was remobilised (Fig. 6) despite the increase in Eh and decrease in the percentage of 0.5 N HCl extractable iron as Fe(II) indicating that soil oxidation occurred. This minor remobilisation may be attributable to either desorption of Cr(VI) or oxidation of Cr(III). The pH drop observed during soil oxidation can be attributed to both the oxidation and the hydrolysis of Fe minerals, which consume OH^- [45], and the development of a carbonate buffered system due to dissolution of atmospheric CO_2. As CrO_4^{2-} adsorbs strongly to surfaces at pH values below 8 [46], measurement of the concentration in the aqueous phase will have slightly underestimated the amount of Cr(VI) in the system. However the amount of Cr(VI) present in the soil after oxidation for 60 days is too low to be detected by XAS (Fig. 2). Also the EXAFS spectra from the oxidised experimental sample is fitted best by the same 3 shell Fe(Cr) model as the other soil samples. This indicates that the majority of the Cr remains in the same coordination environment in the solid phase. This is consistent with the work of others who have shown that Cr(III) is not readily reoxidised in air alone [47]. Mn oxides are known to be more effective oxidising agents for Cr(III) [48], but this is not an immediate concern at the study site as any Mn-oxides present would probably have been reduced during the development of microbial anoxia that resulted in Fe(II) accumulation in soils [12]. The lack of reactivity suggests that once Cr has accumulated in the soils beneath the waste, it is in a form that is resistant to remobilisation via air oxidation.

4.6. Implications for managing legacy COPR waste sites

For the site reported here, the presence of a layer of Fe(II)-containing sandy clay beneath the waste seems to have two beneficial outcomes. Firstly, it acts as an aquitard reducing the water flux from the waste into the aquifer below. Instead, contaminated water at this site is directed to surface discharge, where there is at least an opportunity to intercept and treat it (currently much of the water from the COPR drains into a ditch along the southern boundary; Fig. 1a). Secondly, reaction of Cr(VI) with soil associated Fe(II) within the clay layer produces a Cr(III)–Fe(III) oxy-hydroxide precipitate that is resistant to oxic remobilisation, significantly reducing the downward migration of Cr(VI).

The presence of a Fe(II)-containing soil beneath the waste may seem fortuitous and site specific in nature, but it appears to be the result of a common metabolic process in soil microorganisms and is driven by natural soil organic matter. At a COPR site in New Jersey [49] it was observed that a anoxic, organic-rich soil horizon directly beneath the waste also prevented Cr(VI) migration from the COPR into underlying aquifers. It therefore seems likely that reductive precipitation of Cr(VI) by soil associated Fe(II) also occurred at that site. Site investigations of COPR contaminated land should therefore determine the redox state of the subsurface below the waste and assess if Fe(II)-containing soils are present and can act as natural "reactive barriers" for Cr(VI) contaminated water. In addition, even where unfavourable oxidising conditions exist, populations of alkali and Cr(VI) tolerant Fe(III)-reducing bacteria are often present [22] and it may be possible to induce *in situ* microbial Fe(III)-reduction (e.g. by addition of electron donors) to produce Fe(II) in the soil, and thus attenuate Cr(VI) migration.

5. Conclusions

Cr(VI) is migrating with water from the legacy COPR tip into the underlying soil layers. Chromium is accumulating in these soils predominately in its reduced Cr(III) form within a mixed Cr(III)–Fe(III) oxy-hydroxide phase which is resistant to air oxidation. The soil directly beneath the waste is sub-oxic, with a substantial proportion of the microbial available iron as Fe(II), and it contains an indigenous microbial population capable of reducing iron from Fe(III) to Fe(II). Thus this study suggests that Cr(VI) derived from the highly alkaline COPR can be effectively sequestered in the soil beneath the waste through reduction by microbially produced soil associated Fe(II), and this results in co-precipitation as Cr(III) within a stable Fe(III) oxide host phase.

Supporting information

Supporting online material provides further details about experimental procedures and 16 s rRNA sequence analysis (Sections 1–4), as well as a detailed tables of XRF analytical results (Tables S1), phylogenetic assignments (Tables S2 and S3), B2-310 soil sample backscatter SEM image (Fig. S1) and EDX spectra from STEM analysis (Fig. S2). The EXAFS spectra and coordination structure of chromite ore are also given (Table S4 and Fig. S3).

Acknowledgements

RAW is funded by a University of Leeds, John Henry Garner Scholarship. Thanks to: Dr. Phil Studds and Mark Bell, Ramboll UK, for enabling field work; Dr. Eric Condliffe, University of Leeds, for support during SEM analysis; and Prof. Fred Mosselmans for advice during STFC funded EXAFS experiments at the Diamond Light Source.

Appendix A. Supplementary data

Supplementary data associated with this article can be found, in the online version, at doi:10.1016/j.jhazmat.2011.07.067.

References

[1] G. Darrie, Commercial extraction technology and process waste disposal in the manufacture of chromium chemicals from ore, Environ. Geochem. Health 23 (2001) 187–193.
[2] D. Deakin, L.J. West, D.I. Stewart, B.W.D. Yardley, Leaching behaviour of a chromium smelter waste heap, Waste Manage. 21 (2001) 265–270.
[3] J.S. Geelhoed, J.C.L. Meeussen, S. Hillier, D.G. Lumsdon, R.P. Thomas, J.G. Farmer, E. Paterson, Identification and geochemical modeling of processes controlling leaching of Cr(VI) and other major elements from chromite ore processing residue, Geochim. Cosmochim. Acta 66 (2002) 3927–3942.
[4] J.S. Geelhoed, J.C.L. Meeussen, M.J. Roe, S. Hillier, R.P. Thomas, J.G. Farmer, E. Paterson, Chromium remediation or release? Effect of iron(II) sulfate addition on chromium(VI) leaching from columns of chromite ore processing residue, Environ. Sci. Technol. 37 (2003) 3206–3213.
[5] D.I. Stewart, I.T. Burke, R.J.G. Mortimer, Stimulation of microbially mediated chromate reduction in alkaline soil-water systems, Geomicrobiol. J. 24 (2007) 655–669.
[6] USEPA, Toxicological Review of Hexavalent Chromium, 1998, http://www.epa.gov/ncea/iris.
[7] A. Broadway, M.R. Cave, J. Wragg, F.M. Fordyce, R.J.F. Bewley, M.C. Graham, B.T. Ngwenya, J.G. Farmer, Determination of the bioaccessibility of chromium in Glasgow soil and the implications for human health risk assessment, Sci. Total Environ. 409 (2010) 267–277.
[8] A. Pechova, L. Pavlata, Chromium as an essential nutrient: a review, Vet. Med-Czech 52 (2007) 1–18.
[9] F.C. Richard, A.C. Bourg, Aqueous geochemistry of Cr: a review, Water Res. 25 (1991) 807–816.
[10] D. Rai, B.M. Sass, D.A. Moore, Chromium(III) hydrolysis constants and solubility of chromium(III) hydroxide, Inorg. Chem. 26 (1987) 345–349.
[11] C.J. Lin, The chemical transformations of chromium in natural waters – a model study, Water Air Soil Pollut. 139 (2002) 137–158.
[12] D.R. Lovley, Dissimilatory Fe(III) and Mn(IV) reduction, Microbiol. Rev. 55 (1991) 259–287.

[13] D.R. Lovley, Microbial Fe(III) reduction in subsurface environments, FEMS Microbiol. Rev. 20 (1997) 305–313.
[14] J. Pollock, K.A. Weber, J. Lack, L.A. Achenbach, M.R. Mormile, J.D. Coates, Alkaline iron(III) reduction by a novel alkaliphilic, halotolerant, Bacillus sp isolated from salt flat sediments of Soap Lake, Appl. Microbiol. Biotechnol. 77 (2007) 927–934.
[15] D.G. Zavarzina, T.V. Kolganova, E.S. Boulygina, N.A. Kostrikina, T.P. Tourova, G.A. Zavarzin, Geoalkalibacter ferrihydriticus gen. nov sp nov., the first alkaliphilic representative of the family Geobacteraceae, isolated from a soda lake, Microbiologica 75 (2006) 673–682.
[16] S.E. Fendorf, Surface-reactions of chromium in soils and waters, Geoderma 67 (1995) 55–71.
[17] C.M. Hansel, S.G. Benner, S. Fendorf, Competing Fe(II)-induced mineralization pathways of ferrihydrite, Environ. Sci. Technol. 39 (2005) 7147–7153.
[18] A. Rehman, A.R. Shakoori, Heavy metal resistance Chlorella spp., isolated from tannery effluents, and their role in remediation of hexavalent chromium in industrial waste water, Bull. Environ. Contam. Toxicol. 66 (2001) 542–547.
[19] A. Rehman, A. Zahoor, B. Muneer, S. Hasnain, Chromium tolerance and reduction potential of a Bacillus sp.ev3 isolated from metal contaminated wastewater, Bull. Environ. Contam. Toxicol. 81 (2008) 25–29.
[20] K. Horikoshi, Alkaliphiles, Proc. Jpn. Acad. A-Phys. 80 (2004) 166–178.
[21] D.I. Stewart, I.T. Burke, D.V. Hughes-Berry, R.A. Whittleston, Microbially mediated chromate reduction in soil contaminated by highly alkaline leachate from chromium containing waste, Ecol. Eng. 36 (2010) 211–221.
[22] R.A. Whittleston, D.I. Stewart, R.J.G. Mortimer, D.J. Ashley, I.T. Burke, Effect of microbially induced anoxia on Cr(VI) mobility at a site contaminated with hyperalkaline residue from chromite ore processing, Geomicrobiol. J. 28 (2011) 68–82.
[23] B.A. Schumacher, Methods for the Determination of Total Organic Carbon (TOC) in Soils and Sediments, United States Environmental Protection Agency, Las Vegas, 2002.
[24] ASTM, D4972-01: standard test method for pH of soils Annual Book of ASTM Standards, vol. 4, American Society for Testing and Materials, 2006, pp. 963–965.
[25] R.J. Vitale, G.R. Mussoline, J.C. Petura, B.R. James, Cr(VI) soil analytical method: a reliable analytical method for extracting and quantifying Cr(VI) in soils, J. Soil Contam. 6 (1997) 581–593.
[26] USEPA, SW-846 Manual: Method 7196. Chromium Hexavalent (Colorimetric), 1992, Retrieved 6th January 2006.
[27] E. Viollier, P.W. Inglett, K. Hunter, A.N. Roychoudhury, P. Van Cappellen, The ferrozine method revisited: Fe(II)/Fe(III) determination in natural waters, Appl. Geochem. 15 (2000) 785–790.
[28] I.T. Burke, C. Boothman, J.R. Lloyd, F.R. Livens, J.M. Charnock, J.M. McBeth, R.J.G. Mortimer, K. Morris, Reoxidation behavior of technetium, iron, and sulfur in estuarine sediments, Environ. Sci. Technol. 40 (2006) 3529–3535.
[29] K.A. Weber, F.W. Picardal, E.E. Roden, Microbially catalyzed nitrate-dependent oxidation of biogenic solid-phase Fe(II) compounds, Environ. Sci. Technol. 35 (2001) 1644–1650.
[30] D.R. Lovley, E.J.P. Phillips, Availability of ferric iron for microbial reduction in bottom sediments of the fresh-water tidal Potomac river, Appl. Environ. Microbiol. 52 (1986) 751–757.
[31] I.P. Saraswat, A.C. Vajpei, Characterization of chromium-oxide hydrate gel, J. Mater. Sci. Lett. 3 (1984) 515–517.
[32] Q. Wang, G.M. Garrity, J.M. Tiedje, J.R. Cole, Naive Bayesian classifier for rapid assignment of rRNA sequences into the new bacterial taxonomy, Appl. Environ. Microbiol. 73 (2007) 5261–5267.
[33] J.G. Parsons, K. Dokken, I.R. Peralta-Videa, J. Romero-Gonzalez, J.L. Gardea-Torresdey, X-ray absorption near edge structure and extended X-ray absorption fine structure analysis of standards and biological samples containing mixed oxidation states, of chromium(III) and chromium(VI), Appl. Spectrosc. 61 (2007) 338–345.
[34] M.L. Peterson, G.E. Brown, G.A. Parks, Direct XAFS evidence for heterogeneous redox reaction at the aqueous chromium/magnetite interface, Colloid Surf. A-Physicochem. Eng. Asp. 107 (1996) 77–88.
[35] Y.T. He, C.C. Chen, S.J. Traina, Inhibited Cr(VI) reduction by aqueous Fe(II) under hyperalkaline conditions, Environ. Sci. Technol. 38 (2004) 5535–5539.
[36] J. Atkins, Modelling groundwater and chromite migration through an old spoil tip in Copley, MSc Dissertation, School of Earth and Environment, University of Leeds, Leeds, UK, 2009.
[37] J.M. Tinjum, C.H. Benson, T.B. Edil, Mobilization of Cr(VI) from chromite ore processing residue through acid treatment, Sci. Total Environ. 391 (2008) 13–25.
[38] E. Doelsch, I. Basile-Doelsch, J. Rose, A. Masion, D. Borschneck, J.L. Hazemann, H. Saint Macary, J.Y. Borrero, New combination of EXAFS spectroscopy and density fractionation for the speciation of chromium within an andosol, Environ. Sci. Technol. 40 (2006) 7602–7608.
[39] M.L. Peterson, A.F. White, G.E. Brown, G.A. Parks, Surface passivation of magnetite by reaction with aqueous Cr(VI): XAFS and TEM results, Environ. Sci. Technol. 31 (1997) 1573–1576.
[40] W.D. Derbyshire, H.J. Yearian, X-ray diffraction and magnetic measurements of the Fe–Cr spinels, Phys. Rev. 112 (1958) 1603–1607.
[41] L. Charlet, A. Manceau, X-ray absorption spectroscopic study of the sorption of Cr(Iii) at the oxide water interface. 2. Adsorption, coprecipitation, and surface precipitation on hydrous ferric-oxide, J. Colloid Interface Sci. 148 (1992) 443–458.
[42] J. Frommer, M. Nachtegaal, I. Czekaj, R. Kretzschmar, The Cr X-ray absorption K-edge structure of poorly crystalline Fe(III)–Cr(III)–oxyhydroxides, Am. Mineral. 95 (2010) 1202–1213.
[43] I. Tiago, A.P. Chung, A. Verissimo, Bacterial diversity in a nonsaline alkaline environment: heterotrophic aerobic populations, Appl. Environ. Microbiol. 70 (2004) 7378–7387.
[44] P. Stougaard, F. Jorgensen, M.G. Johnsen, O.C. Hansen, Microbial diversity in ikaite tufa columns: an alkaline cold ecological niche in Greenland, Environ. Microbiol. 4 (2002) 487–493.
[45] R.M. Cornell, U. Schwertmann, The Iron Oxides: Structure, Properties, Reactions, Occurrences and Uses, 2nd ed., Wiley-VCH, Weinheim, 2003.
[46] D. Langmuir, Adsorption–desorption reactions, in: Aqueous Environmental Geochemistry, Prentice-Hall, Inc., Upper Saddle River, NJ, 1997, p. 371.
[47] D.C. Schroeder, G.F. Lee, Potential transformations of chromium in natural-waters, Water Air Soil Pollut. 4 (1975) 355–365.
[48] J.G. Kim, J.B. Dixon, C.C. Chusuei, Y.J. Deng, Oxidation of chromium(III) to (VI) by manganese oxides, Soil Sci. Soc. Am. J. 66 (2002) 306–315.
[49] T.E. Higgins, A.R. Halloran, M.E. Dobbins, A.J. Pittignano, In situ reduction of hexavalent chromium in alkaline soils enriched with chromite ore processing residue, Japca J. Air. Waste Manage. 48 (1998) 1100–1106.